

Tetracopper(I) phosphonitocavitand: synthesis, halide anion inclusion and optical nonlinearity

Qian-Feng Zhang^{a,b,*}, Richard D. Adams^b, Dieter Fenske^c

^aDepartment of Chemistry and Chemical Engineering, Anhui University of Technology, Maanshan, Anhui 243002, China

^bDepartment of Chemistry and Biochemistry and the USC Nanocenter, University of South Carolina, Columbia, SC 29208, USA

^cInstitut für Anorganische Chemie, Universität Karlsruhe, 76128 Karlsruhe, Germany

Received 19 January 2005; revised 1 February 2005; accepted 3 February 2005

Available online 9 March 2005

Abstract

Treatment of tetraphosphonitoresorcinarene $[(\text{CH}_3)_2\text{CHCH}_2\text{CHC}_6\text{H}_2\text{O}_2\text{PPh}]_4$ (**1**) with an excess $[\text{CuCl}]$ powder in the presence of pyridine (py) yielded a tetracopper(I) phosphonitocavitand $[\text{pyH}][\text{I} \cdot \text{Cu}_4(\mu\text{-Cl})_4(\mu_4\text{-Cl})]$ (**2**). The Included $\mu_4\text{-Cl}$ in **2** was easily substituted by heavy halide anion to give $[\text{pyH}][\text{I} \cdot \text{Cu}_4(\mu\text{-Cl})_4(\mu_4\text{-X})]$ ($\text{X} = \text{Br}$, **3**; I , **4**). The complexes **2**, **3**, and **4** have been characterized by X-ray structure determinations. The similar structure contains four coplanar copper atoms bridged by four $\mu\text{-Cl}$ and one central trapped $\mu_4\text{-X}$ atoms in the inside of the closing bowl-shaped cavitant. The third-order nonlinear optical properties of **2** as a typical metal-cavitand complex were investigated in this paper.

© 2005 Elsevier B.V. All rights reserved.

Keywords: Copper(I); Phosphonitocavitand; Crystal structure; Optical nonlinearity; Supramolecular chemistry

1. Introduction

Supramolecular host–guest complexes constructed from cone-shaped polyaromatic macrocycles such as calixarenes and resorcinarenes including the related cavitants have attracted intensive interests because of their applications in field as diverse ion sensors, storage, transports, and optical electronics [1,2]. The host–guest chemistry for shape- and size-selectivity has also potential application in catalysis reactions [3]. A recent aspect of this interesting chemistry is the confinement of molecules within supramolecular capsules, which are from the assembly of six resorcin[4]-arenes and pyrogallol[4]arenes, with the cavities of the host molecules directed inwards [4–6]. The interior of molecular capsules can be regarded as a ‘new phase of matter’ [7]. A detailed understanding of the interplay and orientation of the host and guest molecules is restricted to the building

block molecules. Among the several building blocks employed [8], resorcinarenes and resorcinarene-based cavitants have proven to be particularly interesting as multidentate ligands, due to the presence of rigidly preorganized cavities of molecular dimensions and the possibility of introducing many different ligand moieties [9]. Thus, the use of these compounds, properly functionalized at the upper rim, has resulted in the formation coordination cages and metal complexes with peculiar anion complexation properties [10].

The functionalized resorcinarene-based molecules as the multidentate bowl-shaped ligands have been recently used to coordinate the surface of metal clusters so as to stabilize the metal cluster and to control the sizes of the resultant nanometer particles [11]. In particular, the affinity of thioated and phosphorylated cavitant ligands towards soft metal ions was demonstrated with the coinage-metal copper(I), silver(I) and gold(I) [10,12,13]. Puddephatt and coworkers have studied interactions of tetraphosphonitoresorcinarene with the coinage-metal Cu^+ , Ag^+ , and Au^+ and reported successively a number of tetrametallophosphonitocavitand complexes, in which the metals occupy in the inside of the closing bowl-shaped cavitant [13–16]. As a part of our research on the third-order nonlinear optical properties (NLO) of coinage-metallic complexes

* Corresponding author. Address: Department of Chemistry and Chemical Engineering, Anhui University of Technology, Maanshan, Anhui 243002, China. Tel.: +86 555 2400 551; fax: +86 555 2400 552.
E-mail address: zhangqf@ahut.edu.cn (Q.-F. Zhang).

and clusters [17], we are interested to the metal complexes by the coordination of functional resorcinarene ligands with coinage-metal atoms. It is expected to find new NLO materials with super-cage and nano-meteric metal complexes stabilized by functionalized molecular capsules. In this paper, we report the syntheses, molecular structures and nonlinear optical properties of tetracopper(I) phosphonitocavitands.

2. Experimental

2.1. General

All manipulations were conducted using Schlenk techniques under an atmosphere of nitrogen. Phosphonitocavitand [*rccc*-2,8,14,20-Tetrakis-(*iso*-butyl)-phosphonitocavitand (C₄₄H₄₈O₈P₄Ph₄)] (**1**) was prepared by a modification of the literature method [13]. IR spectrum was measured on a Digilab FTS-40 spectrophotometer. Electronic spectrum was performed on an Hitachi U-3410 spectrophotometer. ³¹P NMR spectrum was recorded on a Varian Unity-300 spectrometer relative to 85% H₃PO₄ acid. Mass spectra were obtained on a Finnigan TSQ-700 spectrometer.

2.1.1. Synthesis of [pyH][I·Cu₄(μ-Cl)₄(μ₄-Cl)] (**2**)

A mixture of excess CuCl powder (100 mg, 1.0 mmol), **1** (170 mg, 0.15 mmol) and py (1.0 ml) in CH₂Cl₂ (25 ml) was stirred at room temperature overnight. The resulting light yellow solution was filtered to remove the unreacted CuCl. The solvent was pumped off and the residue was recrystallized from CH₂Cl₂/MeOH. Needle colorless crystals suitable for X-ray diffraction were obtained for several days. Yield: 186 mg, 91%. Anal. Found: C, 51.6; H, 4.41; N, 1.49%. Calcd for C₇₃H₇₄NO₈P₄Cl₅Cu₄·CH₃CN·CH₂Cl₂: C, 52.4; H, 4.45; N, 1.58%. UV-Vis (CH₂Cl₂, nm): 292(s), 308(sh), 447(br). ³¹P NMR (CDCl₃, ppm): δ 132.7 (s, br). MS (FAB): *m/z* 1599 (**2**-pyH).

2.1.2. Synthesis of [pyH][I·Cu₄(μ-Cl)₄(μ₄-Br)] (**3**)

To a solution of **2** (117 mg, 0.07 mmol) in THF (10 ml) was added a solution of NaBr (50 mg, 0.49 mmol) in water (1 ml), and then the mixture was stirred 2 h. The solvent was pumped off and the residue was washed with MeOH and Et₂O. Recrystallization from CH₂Cl₂/MeOH gave colorless crystals in a yield of 76% (89 mg). Anal. Found: C, 51.2; H, 4.47; N, 0.93%. Calcd for C₇₃H₇₄NO₈P₄Cl₄BrCu₄·CH₃OH: C, 51.5; H, 4.52; N, 0.81%. UV-Vis (CH₂Cl₂, nm): 302(s), 316(sh), 445(br). ³¹P NMR (CDCl₃, ppm): δ 129.5 (s, br). MS (FAB): *m/z* 1614 (**3**-pyH).

2.1.3. Synthesis of [pyH][I·Cu₄(μ-Cl)₄(μ₄-I)] (**4**)

This complex was prepared similarly as for **3** using NaI (70 mg, 0.47 mmol) in place of NaBr, and recrystallized from CH₂Cl₂/MeOH. Yield: 82 mg, 72%. Anal. Found: C,

50.6; H, 4.36; N, 0.83%. Calcd for C₇₃H₇₄NO₈P₄Cl₄·ICu₄·CH₃OH: C, 50.1; H, 4.40; N, 0.79%. UV-Vis (CH₂Cl₂, nm): 305(s), 318(sh), 451(br). ³¹P NMR (CDCl₃, ppm): δ 118.9 (s, br). MS (FAB): *m/z* 1661 (**4**-pyH).

2.2. Crystal structure determination

Single crystals of complexes **2**·CH₃CN·CH₃OH, **3**·CH₃OH and **4**·CH₃OH were obtained from the methanol diffuse into their CH₂Cl₂ solutions. Each of single crystal was quickly sealed inside a capillary with mother liquor to prevent loss solvents in the crystal lattice. X-ray intensity data were collected on a Bruker SMART APEX 1000 CCD area-detecting diffractometer equipped with graphite monochromated Mo Kα radiation (λ = 0.71073 Å) by using an ω scan technique at room temperature. The collected frames were processed with the software SAINT [18]. The data was corrected for absorption using the program SADABS [19]. The structure was solved by direct methods using the SHELXTL software package [20]. All heavy atoms positions (Cu, I, Br, Cl and P) were revealed on the first refinement. Other nonhydrogen atoms were located from subsequent difference Fourier syntheses. The structure was refined by full-matrix least-squares method on *F*². All nonhydrogen atoms were refined anisotropically. Hydrogen atoms were included but not refined. The pyridine rings in **3**·CH₃OH and **4**·CH₃OH were refined with the bond distance restraint due to disorders. Further details of the structure analyses are listed in Table 1. Selected bond lengths and angles of compounds **2**·CH₃CN·CH₃OH, **3**·CH₃OH and **4**·CH₃OH are given in Table 2.

2.3. Optical measurements

A CH₃CN solution of 7.5 × 10⁻³ mol dm⁻³ of complex **2** was placed in a 1-mm quartz cell for optical measurements. The optical limiting characteristics along with nonlinear absorption and refraction was investigated with a linearly polarized laser light (λ = 532 nm, pulse width = 7 ns) generated from a Q-switched and frequency-doubled Nd:YAG laser. The spatial profiles of the optical pulses were nearly Gaussian. The laser beam was focused with a 25-cm focal-length focusing mirror. The radius of the laser beam waist was measured to be 30 ± 5 μm (half-width at 1/e² maximum in irradiance). The incident and transmitted pulse energy were measured simultaneously by two Laser Precision detectors (RjP-735 energy probes) communicating to a computer via an IEEE interface [21], while the incident pulse energy was varied by a Newport Com. Attenuator. The interval between the laser pulses was chosen to be 1 s to avoid the influence of thermal and long-term effects. The details of the set-up can be found elsewhere [22].

Table 1

Crystal data and structure refinements for **1**·CH₃CN·CH₂Cl₂, **2**·CH₃OH, and **3**·CH₃OH

| Compound | 1 ·CH ₃ CN· CH ₂ Cl ₂ | 2 ·CH ₃ OH | 3 ·CH ₃ OH |
|---|---|---|--|
| Empirical formula | C ₇₆ H ₇₉ N ₂ O ₈ - P ₄ Cl ₇ Cu ₄ | C ₇₄ H ₇₈ NO ₉ P ₄ - Cl ₄ BrCu ₄ | C ₇₄ H ₇₈ NO ₉ P ₄ - Cl ₄ ICu ₄ |
| Formula weight | 1774.60 | 1725.12 | 1772.11 |
| Crystal system | Monoclinic | Monoclinic | Monoclinic |
| Space group | <i>P</i> 2 ₁ / <i>n</i> | <i>P</i> 2 ₁ / <i>n</i> | <i>P</i> 2 ₁ / <i>n</i> |
| <i>a</i> (Å) | 20.711(2) | 20.8253(18) | 20.8459(14) |
| <i>b</i> (Å) | 19.4586(19) | 19.5146(16) | 19.5462(13) |
| <i>c</i> (Å) | 20.766(2) | 20.8325(19) | 20.8371(12) |
| β (deg) | 105.683(2) | 105.695(2) | 105.541(2) |
| Volume (Å ³) | 8057.3(14) | 8150.6(12) | 8179.8(9) |
| <i>Z</i> | 4 | 4 | 4 |
| <i>T</i> (K) | 173 | 294 | 294 |
| Density (calcd) (g/cm ³) | 1.463 | 1.406 | 1.299 |
| Absorption coefficient (mm ⁻¹) | 1.406 | 1.781 | 1.663 |
| <i>F</i> (000) | 3632 | 3520 | 3592 |
| θ range for data collection (deg) | 1.46–25.03 | 1.46–25.03 | 1.45–25.03 |
| Reflections collected | 47485 | 48633 | 48708 |
| Independent reflections | 14221 | 14371 | 14428 |
| <i>R</i> (int) | 0.0735 | 0.0956 | 0.1147 |
| Data/restraints/ parameters | 14221/6/879 | 14371/0/834 | 14428/0/850 |
| Goodness of fit on <i>F</i> ² | 0.935 | 0.979 | 1.072 |
| Final <i>R</i> ¹ , <i>wR</i> ² ^b | 0.0692, 0. | 0.0753, 0. | 0.0857, 0. |
| [<i>I</i> > 2σ(<i>I</i>)] (all data) | 1455, 0.1089, 0.1899 | 1555, 0.1610, 0.2436 | 1507, 0.1575, 0.2235 |
| Final diff. features (e/Å ³) | 1.058, -0.628 | 1.176, -0.790 | 1.558, -1.751 |

$$^a R1 = \sum |F_o| - |F_c| / \sum |F_o|.$$

$$^b wR2 = [\sum w(|F_o^2| - |F_c^2|)^2 / \sum w|F_o^2|]^2.$$

3. Results and discussion

The bowl-shaped phosphonitocavitand (**1**) with four PhP units was easily obtained by treatment of resorcin[4]arene with phosphonous dichloride PhPCl₂ in the presence of pyridine (py) as base [13]. Similar to silver analogue of phosphonitocavitand [23], treatment of ligand **1** in CH₂Cl₂ solution with an excess [CuCl] powder in the presence of py gave the sole compound tetracopper(I) phosphonitocavitand [pyH][**1**·Cu₄(μ-Cl)₄(μ₄-Cl)] (**2**) as colorless crystals. Complex **2** can be dissolved in most polar solvents, such as THF, CH₂Cl₂ and acetone. Reaction of **2** with NaBr or NaI in THF solution gave new complex [pyH][**1**·Cu₄(μ-Cl)₄(μ₄-X)] (X=Br, **3**; I, **4**). The heavy halide Br⁻ and I⁻ substituted the μ₄-Cl⁻ anion to form the face-bridging μ₄-Br and μ₄-I bindings, respectively. Attempts to replace all the μ-Cl groups by using excess heavy halide resource and long reaction time failed, indicative of the Cu₄(μ-Cl)₄ having a fixed crown structure. Thus, the cavity size of the Cu₄(μ-Cl)₄ crown structure may be optimized for the

Table 2

Selected bond lengths (Å) and angles (deg) for **1**·CH₃CN·CH₂Cl₂, **2**·CH₃OH, and **3**·CH₃OH

| | X=Cl (1) | X=Br (2) | X=I (3) |
|-------------------|-------------------|-------------------|------------------|
| Cu(1)–P(1) | 2.169(2) | 2.181(4) | 2.175(4) |
| Cu(2)–P(2) | 2.168(2) | 2.173(4) | 2.178(4) |
| Cu(3)–P(3) | 2.169(2) | 2.177(4) | 2.195(4) |
| Cu(4)–P(4) | 2.170(2) | 2.173(4) | 2.192(4) |
| Cu(1)–Cl(1) | 2.358(2) | 2.399(3) | 2.380(5) |
| Cu(1)–Cl(4) | 2.353(2) | 2.399(3) | 2.352(4) |
| Cu(2)–Cl(1) | 2.347(2) | 2.405(3) | 2.355(4) |
| Cu(2)–Cl(2) | 2.345(2) | 2.396(3) | 2.385(5) |
| Cu(3)–Cl(2) | 2.347(2) | 2.383(3) | 2.366(4) |
| Cu(3)–Cl(3) | 2.349(2) | 2.443(3) | 2.534(4) |
| Cu(4)–Cl(3) | 2.353(2) | 2.438(3) | 2.533(4) |
| Cu(4)–Cl(4) | 2.351(2) | 2.390(3) | 2.359(5) |
| Cu(1)–X | 2.551(2) | 2.667(2) | 2.773(2) |
| Cu(2)–X | 2.579(2) | 2.669(2) | 2.771(2) |
| Cu(3)–X | 2.580(2) | 2.645(2) | 2.757(2) |
| Cu(4)–X | 2.557(2) | 2.646(2) | 2.755(2) |
| P(1)–Cu(1)–Cl(1) | 113.55(8) | 117.02(13) | 118.37(17) |
| P(1)–Cu(1)–Cl(4) | 117.12(8) | 113.87(14) | 114.21(17) |
| Cl(4)–Cu(1)–Cl(1) | 104.02(8) | 104.49(12) | 103.99(16) |
| P(1)–Cu(1)–X | 127.79(7) | 123.26(12) | 120.06(12) |
| Cl(4)–Cu(1)–X | 94.36(7) | 97.84(10) | 98.97(12) |
| Cl(1)–Cu(1)–X | 95.66(7) | 96.99(9) | 98.07(12) |
| P(2)–Cu(2)–Cl(2) | 115.41(9) | 113.91(13) | 113.96(17) |
| P(2)–Cu(2)–Cl(1) | 113.01(8) | 116.94(14) | 118.56(17) |
| Cl(2)–Cu(2)–Cl(1) | 107.58(8) | 104.65(12) | 104.12(16) |
| P(2)–Cu(2)–X | 126.32(7) | 123.45(12) | 119.97(12) |
| Cl(2)–Cu(2)–X | 96.22(7) | 97.72(10) | 99.06(12) |
| Cl(1)–Cu(2)–X | 95.18(7) | 96.79(9) | 98.04(12) |
| P(3)–Cu(3)–Cl(2) | 115.28(8) | 111.86(14) | 112.88(17) |
| P(3)–Cu(3)–Cl(3) | 113.07(8) | 113.89(13) | 112.79(15) |
| Cl(2)–Cu(3)–Cl(3) | 107.70(8) | 107.17(12) | 106.81(14) |
| P(3)–Cu(3)–X | 126.33(7) | 123.00(12) | 119.12(12) |
| Cl(2)–Cu(3)–X | 96.14(7) | 98.69(9) | 99.95(13) |
| Cl(3)–Cu(3)–X | 95.24(7) | 100.22(9) | 103.85(10) |
| P(4)–Cu(4)–Cl(4) | 117.19(8) | 111.94(14) | 112.85(17) |
| P(4)–Cu(4)–Cl(3) | 113.67(8) | 113.79(13) | 112.49(15) |
| Cl(4)–Cu(4)–Cl(3) | 104.28(7) | 107.05(12) | 106.92(14) |
| P(4)–Cu(4)–X | 127.42(7) | 123.07(12) | 119.26(13) |
| Cl(4)–Cu(4)–X | 94.27(7) | 98.63(10) | 99.99(13) |
| Cl(3)–Cu(4)–X | 95.75(7) | 100.33(9) | 103.94(10) |
| Cu(2)–Cl(1)–Cu(1) | 87.78(7) | 86.76(11) | 88.71(14) |
| Cu(2)–Cl(2)–Cu(3) | 87.05(7) | 86.32(11) | 87.46(14) |
| Cu(3)–Cl(3)–Cu(4) | 87.83(7) | 82.62(10) | 79.43(12) |
| Cu(4)–Cl(4)–Cu(1) | 87.56(7) | 86.17(11) | 87.60(14) |
| Cu(1)–X–Cu(4) | 79.14(6) | 76.01(6) | 72.79(6) |
| Cu(1)–X–Cu(2) | 78.96(6) | 76.40(6) | 72.82(7) |
| Cu(4)–X–Cu(2) | 127.19(7) | 120.72(7) | 113.67(6) |
| Cu(1)–X–Cu(3) | 127.29(7) | 120.71(7) | 113.79(6) |
| Cu(4)–X–Cu(3) | 78.82(6) | 75.04(6) | 71.95(7) |
| Cu(2)–X–Cu(3) | 77.54(6) | 75.93(6) | 72.90(6) |

heavy halides inclusion. The ³¹P NMR resonances for the complexes **2–4** show a single broad peak downfield from that of the free ligand **1** (165.7 ppm), and ³¹P resonances shift upfield on going from Cl⁻ (132.7 ppm) to I⁻ (118.9 ppm), a trend that can again be ascribed to a smooth increase in orbital overlap. The reason for this is that the deshielding effect may result from orbital overlap due to Cu⁺ being a *d*¹⁰ system.

In order to prove the $\text{Cu}_4(\mu\text{-Cl})_4$ crown structure with the halide anion inclusion, the structures of complexes **2**, **3**, and **4** were clearly confirmed by single crystal X-ray diffraction. All crystal structures consist of discrete $[\text{pyH}]^+$ cations and tetracopper(I) phosphonitocavitands along with the lattice solvents. The selected structural parameters for these three complexes are compiled in Table 2 for comparison. The structure of the anion $[\mathbf{1} \cdot \text{Cu}_4(\mu\text{-Cl})_4(\mu_4\text{-Cl})]^-$ in **2** is shown in Fig. 1 as both top and side views. The structures of the anions $[\mathbf{1} \cdot \text{Cu}_4(\mu\text{-Cl})_4(\mu_4\text{-Br})]^-$ in **3** and $[\mathbf{1} \cdot \text{Cu}_4(\mu\text{-Cl})_4(\mu_4\text{-I})]^-$ in **4** are illustrated in Figs. 2 and 3, respectively, from side views. The similar structures of phosphonitocavitand with different cavitand ligands have been previously reported by Puddephatt [14,15]. As expected, the tetraphosphonitocalixarene unit is present in the bowl-shaped conformation with each phosphorous bonded to a copper(I) atom. The $\text{Cu}_4(\mu\text{-Cl})_4(\mu_4\text{-X})$ unit lies in the inside of the closing bowl-shaped cavitand, of which the $\text{Cu}_4(\mu\text{-Cl})_4$ moiety is arranged in a crown shape around the bowl rim, the $\mu_4\text{-X}$ is trapped inside the bowl center.

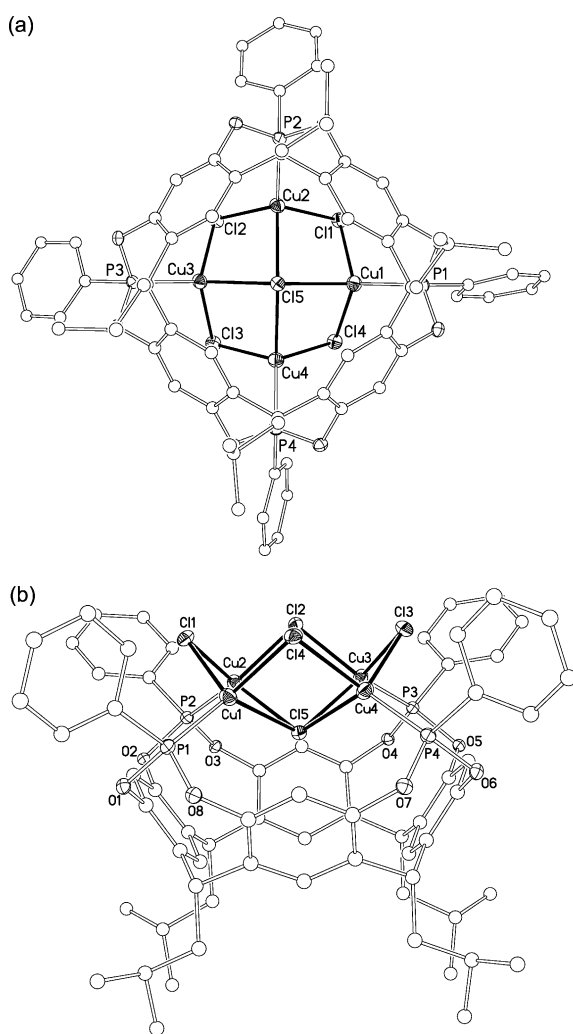


Fig. 1. Perspective view of the anion $[\mathbf{1} \cdot \text{Cu}_4(\mu\text{-Cl})_4(\mu_4\text{-Cl})]^-$ in **2** with the ellipsoids drawn at 30% probability level: (a) top view, (b) side view.

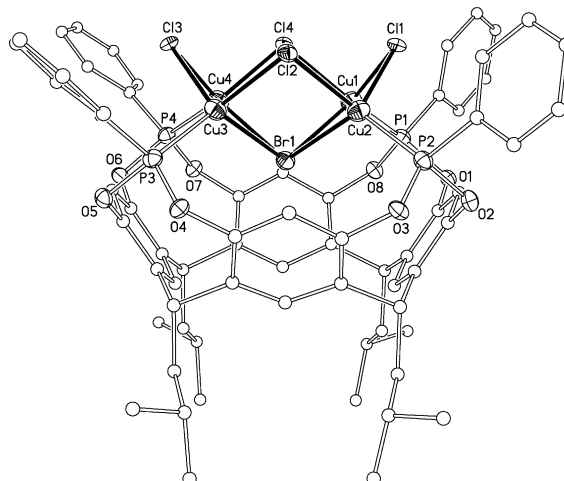


Fig. 2. A perspective view of the anion $[\mathbf{1} \cdot \text{Cu}_4(\mu\text{-Cl})_4(\mu_4\text{-Br})]^-$ in **3** from the side view. The thermal ellipsoids were drawn at 30% probability level.

The $\text{Cu}_4(\mu\text{-Cl})_4(\mu_4\text{-X})$ aggregate approximates to C_{4v} symmetry. Each copper atom is tetrahedrally coordinated, and the four copper atoms are nearly coplanar with an average deviation of 0.01 Å from the least squares plane. Distances from the Cu atoms to $\mu\text{-Cl}$ atoms range from 2.351(2) to 2.534(4) Å, while the $\mu\text{-Cl}-\text{Cu}-\mu\text{-Cl}$ angles range from 103.99(16) to 107.70(8)°. The average value of the $\text{Cu}-\mu_4\text{-Cl}$ interatomic distances is 2.567(2) Å; those of $\text{Cu}-\mu_4\text{-Br}$ and $\text{Cu}-\mu_4\text{-I}$ are 2.657(2) and 2.764(2) Å, respectively, which are obviously shorter than those in the corresponding silver complexes [14,15,23]. The average bond length of $\text{Cu}-\mu_4\text{-X}$ increases from Cl^- to I^- , owing to the increased ionic radii of the halide. A slight difference of the $\text{Cu}-\text{P}$ bond distances is also noted in the three complexes, the average $\text{Cu}-\text{P}$ bond distances are 2.169(2), 2.176(4) and 2.185(4) Å for complexes **2**, **3** and **4**, respectively, suggesting that the $\text{Cu}-\text{P}$ bond interactions are more or less influenced by the inclusion halide anions.

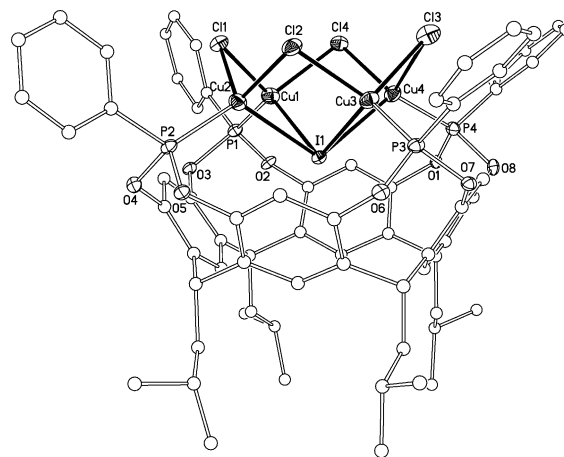


Fig. 3. A perspective view of the anion $[\mathbf{1} \cdot \text{Cu}_4(\mu\text{-Cl})_4(\mu_4\text{-I})]^-$ in **4** from the side view. The thermal ellipsoids were drawn at 30% probability level.

The electronic spectra of complexes **2–4** are characterized by three absorptions in the 284–496 nm range. The high energy absorption may be due to the congregation macrocyclic π -system from phosphonitocavitand ligands. The strong broad peak may be assigned as the internal P-to-Cu charge-transfer. The middle broad at ca. 494 nm may be attributed to metal-to-ligand charge-transfer. The NLO properties of complex **2** as a representative compound were investigated by using the Z-scan technique. The nonlinear absorption component was evaluated under an open aperture configuration. Theoretical curves of transmittance against the Z-position, Eqs. (1) and (2), were fitted to the observed Z-scan data

$$T(Z) = \frac{1}{\pi^{1/2} q(Z)} \int_{-\infty}^{\infty} \ln[1 + q(z)] e^{-z^2} dz \quad (1)$$

$$q(Z) = \alpha_2 I_i(Z) \frac{(1 - e^{-\alpha_0 L})}{\alpha_0} \quad (2)$$

by varying the effective third-order NLO absorptivity α_2 value, where the experimentally measured α_0 (linear absorptivity), L (the optical path of sample) and $I_i(Z)$ (the on-axis irradiance at Z-position) were adopted. The solid line in Fig. 4(a) is the theoretical curve calculated with $\alpha_2 = 1.15 \times 10^{-13}$ m/W for the concentrations 7.5×10^{-3} M for **2** in an acetonitrile solution. The nonlinear refractive component of **2** was assessed by dividing the normalized Z-scan data obtained in the close-aperture configuration by those obtained in the open-aperture configuration. The nonlinear refractive component plotted with the filled squares in Fig. 4(b) was assessed by dividing the normalized Z-scan data obtained under the closed aperture configuration by the normalized Z-scan data obtained under the open aperture configuration. The valley and peak occur at about equal distances from the focus. It can be seen that the difference in valley–peak positions ΔZ_{V-P} is 9.2 mm and the difference between normalised transmittance values at valley and peak positions $\Delta T_{V-P} = 0.22$ for **2**. These results suggest an effectively weak third-order optical nonlinearity [24]. The solid curve is an eye guide for comparison where the effective nonlinear refractivity n_2 value estimated therefore is 3.24×10^{-14} esu for **2**. Comparing the NLO data of complex **2** with the other reported M(W)/Cu(Ag)/S(Se) clusters [17,25], it may be seen that the NLO behavior of complex **2** is slightly inferior to those of polynuclear clusters. Compared with the analogous silver complex [23], the copper complex **2** has relatively weak optical limiting effect. This will make us further to design the synthesis of polynuclear heavy coinage-metal clusters stabilized by phosphonitocavitand ligands. Because the formation of polynuclear clusters with phosphonitocavitands depends very much on the nature of the phosphine and the resource of bridging atoms [26], the present metal complexes with phosphonitocavitand ligands as starting materials may be used to react with active chalcogenide resources. From these

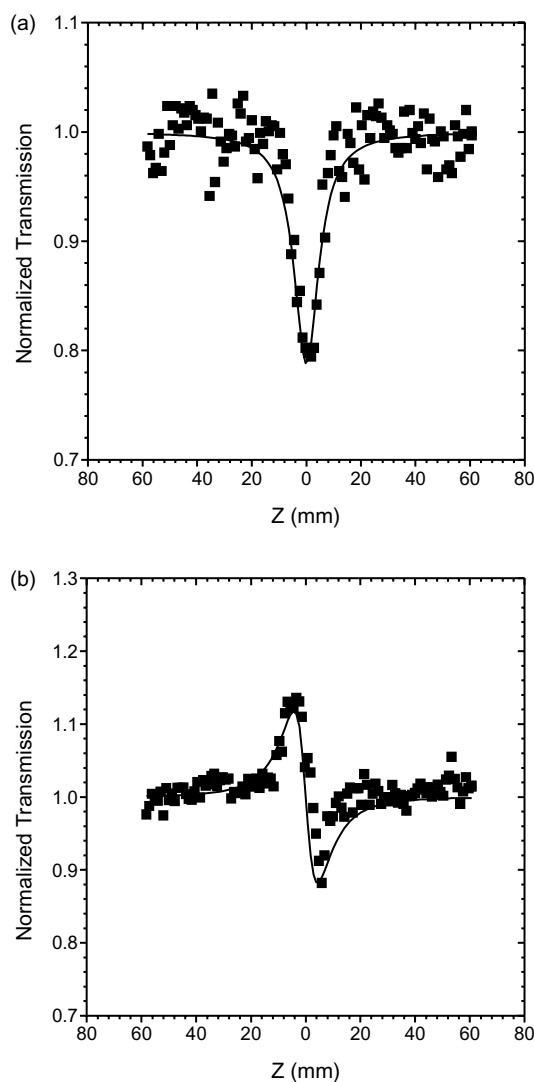


Fig. 4. Z-scan data of 7.5×10^{-3} M of **2** in CH_3CN at 532 nm with I_0 being 1.2×10^{12} W/m^2 : (a) collected under the open aperture configuration showing NLO absorption; (b) obtained by dividing the normalized Z-scan data obtained under the closed aperture configuration by the normalized Z-scan data in (a). The solid curves are theoretical fits based on Z-scan theoretical calculations.

reactions, a variety of structural type polynuclear clusters may be reasonably predicted. Therefore, further studies are in progress, which are directed toward the preparations of polynuclear clusters with phosphonitocavitand ligands so as to obtain desirable nonlinear optical materials.

4. Supplementary materials

Crystal data (excluding structure factors) for the structures in this paper have been deposited with the Cambridge Crystallographic Data Centre as supplementary publication nos. CCDC-254328/254329/254330. These data can be obtained free of charge via www.ccdc.cam.ac.uk/conts/

retrieving.html (or from the Cambridge Crystallographic Data Centre, 12 Union Road, Cambridge CB2 1EZ, UK; fax: (+44) 1223 336 033; or deposit@ccdc.cam.ac.uk).

Acknowledgements

This project was supported by the Key Scientific Research Foundation of State Education Ministry (grant no. 204067) and Anhui Provincial Natural Science Foundation to QFZ. Dr Q.F. Zhang is grateful to the Alexander von Humboldt Foundation for the assistance.

References

- [1] O. Seneque, M.-N. Rager, M. Giorgi, O. Reinaud, *J. Am. Chem. Soc.* 122 (2000) 6128.
- [2] V. Ramanurthy, D.F. Eaton, *Chem. Mater.* 6 (1994) 1128.
- [3] S. Shimizu, S. Shirakawa, Y. Sasaki, C. Hirai, *Angew. Chem. Int. Ed.* 39 (2000) 1256.
- [4] L.R. MacGillivray, J.L. Atwood, *Nature* 389 (1997) 469.
- [5] T. Gerkenmeier, W. Iwanek, C. Agena, R. Fröhlich, S. Kotila, C. Näther, J. Mattay, *Eur. J. Org. Chem.* (1999) 2257.
- [6] J.L. Atwood, L.J. Barbour, A. Jerga, *Chem. Commun.* (2001) 2376.
- [7] A. Shivanyuk, J. Rebek Jr, *Chem. Commun.* (2001) 2374.
- [8] A. Jasat, J.C. Sherman, *Chem. Rev.* 99 (1999) 931 and references therein.
- [9] A.J. Wright, S.E. Matthews, W.B. Fischer, P.D. Beer, *Chem. Eur. J.* 7 (2001) 3474.
- [10] O.D. Fox, M.G.B. Drew, P.D. Beer, *Angew. Chem. Int. Ed.* 39 (2000) 136.
- [11] K.B. Stavens, S.V. Pusztay, S. Zou, R.P. Andres, A. Wei, *Langmuir* 15 (1999) 8337.
- [12] B. Bibal, B. Tinant, J.P. Declercq, J.P. Dutasta, *Chem. Commun.* (2002) 432.
- [13] W. Xu, J.P. Rourke, J.J. Vittal, R.J. Puddephatt, *Inorg. Chem.* 34 (1995) 323.
- [14] W. Xu, J.J. Vittal, R.J. Puddephatt, *J. Am. Chem. Soc.* 115 (1993) 6456.
- [15] W. Xu, J.J. Vittal, R.J. Puddephatt, *J. Am. Chem. Soc.* 117 (1995) 8362.
- [16] W. Xu, J.J. Vittal, R.J. Puddephatt, *Inorg. Chem.* 36 (1993) 86.
- [17] Q.F. Zhang, W.H. Leung, X.Q. Xin, *Coord. Chem. Rev.* 224 (2002) 35.
- [18] SMART and SAINT+ for Windows NT Version 6.02a. Bruker Analytical X-ray Instruments Inc., Madison, WI, USA, 1998.
- [19] G.M. Sheldrick, SADABS, University of Göttingen, Germany, 1996.
- [20] G.M. Sheldrick: SHELXTL Software Reference Manual. Version 5.1. Bruker AXS Inc., Madison, WI, USA, 1997.
- [21] (a) M. Sheik-Bahae, A.A. Said, E.W. Van Stryland, *Opt. Lett.* 14 (1989) 955;
(b) M. Sheik-Bahae, A.A. Said, T.H. Wei, D.J. Hagan, E.W. Van Stryland, *IEEE J. Quantum Electron.* 26 (1990) 760.
- [22] H.W. Hou, B. Liang, X.Q. Xin, K.B. Yu, P. Ge, W. Ji, S. Shi, *J. Chem. Soc. Faraday Trans.* 92 (1996) 2343.
- [23] S. Miao, W.R. Yao, D.S. Guo, Q.F. Zhang, *J. Mol. Struct.* 660 (2003) 159.
- [24] D.G. Mclean, R.L. Sutherland, M.C. Brant, D.M. Brandelik, P.A. Fleity, T. Pottenger, *Opt. Lett.* 18 (1993) 858.
- [25] H.W. Hou, X.Q. Xin, S. Shi, *Coord. Chem. Rev.* 153 (1996) 25.
- [26] S. Dehnen, A. Eichhöfer, D. Fenske, *Eur. J. Inorg. Chem.* (2002) 279.